THE JOURNAL OF PHYSICAL CHEMISTRY A

 VOLUME 113, NUMBER 36, SEPTEMBER 10, 2009

ARTICLES

Cooperative Effect of Hydrogen-Bonded Chains in the Environment of a $\pi \rightarrow \pi^*$ Chromophore

Georgios Fradelos,[†,§] Jakub W. Kaminski,[†] Tomasz A. Wesolowski,*[,†] and Samuel Leutwyler[‡]

Département de Chimie Physique, Université de Genève, 30 quai Ernest-Ansermet, CH-1211 Genève 4, Switzerland, and Departement für Chemie und Biochemie, Freiestrasse 3, CH-3012 Bern, Switzerland

Received: July 9, 2009

Laser resonant two-photon ionization UV spectra provide clear evidence that the effect of increasing the length of the hydrogen-bonded chain consisting of molecules such as NH_3, H_2O, or CH_3OH on the $\pi \rightarrow \pi^*$ excitations of *cis*-7-hydroxyquinoline (*cis*-7HQ) is strongly cooperative [Thut; et al. *J. Phys. Chem. A* **2008**, *112*, 5566.] A theoretical analysis of the experimental data is provided to identify the origin of this cooperativity for four chains. The computational method to determine the changes of the electronic structure of a molecule due to interactions with its environment uses the nonempirical expression for the embedding potential [Wesolowski; Warshel *J. Phys. Chem.* **1993**, *97*, 8050.] It is concluded that the electronic coupling between the molecules at the ends of the chain, which are hydrogen-bonded to *cis*-7HQ, plays a crucial role in this cooperativity.

Introduction

The nonpairwise interactions between hydrogen-bonded molecules, which are referred to frequently also as cooperativity or nonadditivity, manifest themselves experimentally in various ways (for a general overview of this phenomenon in water clusters, see ref 1). In hydrogen-bonded networks, the increase of the size results usually in the increase of the strength of individual hydrogen bonds and of the proton-donor bond length accompanied by shortening of the donor−acceptor distance. As a consequence, the red shift of the O−H (or N−H) infrared stretching band increases with the increase of the size of the hydrogen-bonded network or chain.[2−7] These effects are fully corroborated by quantum mechanical calculations of linear chains of simple hydrogen-bonded molecules such as HCN, HF, and cyanoacetylene as well as water clusters.[8−13] Chains or wires of hydrogen-bonded H_2O and NH_3 molecules have been the objects of our research[15,16] due to their possible role in the excited-state hydrogen atom-transfer processes in biological systems.[14,15] In ref 16, we study the hydrogen-bonded chains comprising several small molecules, which are attached to the probe chromophore *cis*-7-hydroxyquinoline (*cis*-7HQ), which provides a single H-bond acceptor (N) and a single H-bond donor (OH) site, leading to the formation of H-bonded wires of variable length (see Figure 1).

Both experiment and computer modeling for *cis*-7HQ in various nanosolvent environments comprising molecules that do not absorb in the near-UV show that the spectral shifts of the $\pi \rightarrow \pi^*$ excitations localized in *cis*-7HQ increase with the length of the hydrogen-bonded chain of molecules in the environment.[16] An overall picture emerges from these studies according to which (i) the interactions with a single hydrogen-

* To whom correspondence should be addressed. E-mail: Tomasz.Wesolowski@unige.ch.
[†] Université de Genève.
[‡] Departement für Chemie and Biochemie.
[§] E-mail: Georgios.Fradelos@unige.ch.

10.1021/jp906483z CCC: $40.75
Published on Web 08/18/2009

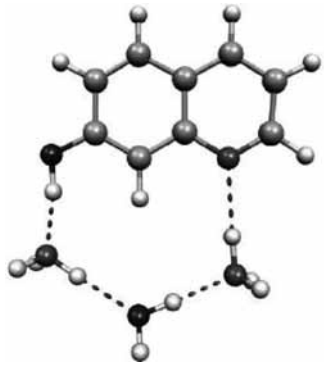

Figure 1. A hydrogen-bonded chain cluster (A···B···C) bound to *cis*-7-hydroxyquinoline (A = NH_3, B = H_2O, C = NH_3). In this work, A and C denote the H-bonded molecules that interact with the OH donor and N acceptor sites of *cis*-7-hydroxyquinoline, respectively.

bonded ligand gives rise to about half of the electronic spectral shift as compared to interactions with two ligands, one attached to the N-site and the other to the OH site and (ii) the addition of the third ligand, which does not interact directly with *cis*-7HQ (see Figure 1), causes further significant increase of the electronic spectral shift.

The overall structure of such three-member chains, although not directly available from experiment, can be reliably obtained from theoretical calculations based on energy minimization and is confirmed by calculations of electronic spectral shifts.[16] According to calculations, the third molecule is positioned in such a way that it links the ligands at the N and OH sites. For this reason, it is referred to as the linker in the present work. The interactions of the lowest-energy $\pi \rightarrow \pi^*$ excitation in *cis*-7HQ with an environment consisting of a single hydrogen-bonded solvent molecule typically lead to a spectral shift $\delta\nu$ in the range from -590 to -905 cm^{-1} (see the experimental data collected in ref 16). Two ligand molecules in the vicinity of O−H and N groups of *cis*-7HQ induce spectral shifts of the $\pi \rightarrow \pi^*$ excitation in the range from -1637 to -1866 cm^{-1}.[16] Introducing a linker molecule B in the middle of the hydrogen-bonded chain results in a further spectral red shift ranging from -315 to -461 cm^{-1}; see ref 16 and also the collection of experimental data in Table 1. This additional shift is denoted by $\delta\delta\nu_B$. The magnitude of $\delta\delta\nu_B$ is quite significant, given that the linker molecule is not hydrogen-bonded to *cis*-7HQ. The overall value of $\delta\delta\nu_B$, the quantity available from both experiments and computer modeling, can be decomposed into the following contributions of a clear physical meaning:

• The direct (through-space) spectral shift induced by the linker molecule. It is defined as the spectral shift due to only one molecule (B), positioned in the same place as in the equilibrium structure of the three-membered chain (ABC). The corresponding contribution to $\delta\delta\nu_B$ is denoted in the present work by $\delta\nu_{B(ABC)}$. The convention is used to denote that the contribution to the total spectral shifts is the following: for $\delta\nu_{X(Y)}$, X specifies the molecule(s) in the environment, whereas Y specifies the chain from which the geometry of X is taken.

• The effect due to the modification of the geometry of the molecules, which are directly hydrogen-bonded to the chromophore (molecules A and C), following the insertion of the linker. The corresponding contribution to the spectral shift $\delta\delta\nu_B$ is denoted by $\delta\delta\nu_{geom}$. It is evaluated as

$$\begin{aligned} \delta\delta\nu_{geom} &= \delta\nu_{AC(ABC)} - \delta\nu_{AC(AC)} \\ &= \nu_{AC(ABC)} - \nu_{AC(AC)} \end{aligned} \quad (1)$$

Note that this contribution arises from both the effects of the change of the intramolecular degrees of freedom of a molecule hydrogen-bonded to *cis*-7HQ as well as the intermolecular degrees of freedom.

• The contribution to the spectral shift resulting from the modification of the electronic structure of the ligands A and C following the insertion of the linker molecule (B) into the *cis*-7HQ + AC system, without any changes in geometry. This term, denoted by $\delta\delta\nu_{el\text{-}coop}$, arises from the electronic coupling between the two ends of the hydrogen-bonded chain. The numerical value of $\delta\delta\nu_{el\text{-}coop}$ cannot be obtained from either experiment or direct theoretical calculations. It is defined as the remainder obtained from subtracting from $\delta\delta\nu_B$ the two contributions $\delta\nu_{B(ABC)}$ and $\delta\delta\nu_{geom}$

$$\delta\delta\nu_{el\text{-}coop} = \delta\delta\nu_B - \delta\nu_{B(ABC)} - \delta\delta\nu_{geom} \quad (2)$$

In the present work, the relative importance of the above three contributions is investigated. The experimental data do not allow one to address this issue directly. We turn, therefore, to the theoretical analysis because it allows one to decompose the calculated values of $\delta\delta\nu_B$.

Orbital-Free Embedding Computations of the Spectral Shifts

The key quantity of interest in this work is the spectral shift induced by the interactions between the chromophore and the molecules hydrogen-bonded to it. The spectral shift is thus a difference between the excitation energies calculated for the same chromophore but for a varying number of molecules in the environment (zero to three in our case). The shifts are rather small (1000 cm^{-1} is just 0.12 eV). Even within the vertical excitation picture of the considered absorption processes, obtaining such shifts from theoretical calculations represents a challenge. Routine application of the "supermolecule strategy", that is, obtaining the shifts as the differences between the excitation energies calculated for the complex and those for the free chromophore, is far from straightforward and prone to various pitfalls. For organic chromophores, the intrinsic accuracy of the electronic excitation energies derived via the linear response time-dependent DFT strategy (LR-TDDFT)[21] is of the same order of magnitude[22] as the spectral shifts considered in the present work. The quality of the shift calculated as a difference of two excitation energies obtained from LR-TDDFT hinges on the assumption that the errors in the excitation energy calculated for the isolated chromophore and that for the chromophore in the complex are the same (or strongly correlated). Unfortunately, for clusters involving organic chromophores and solvent molecules, such a cancellation cannot be assumed. In fact, the opposite has been observed; increasing the size of the cluster leads to the appearance of artificial excitations of no physical meaning.[36] More generally, it is known that the accuracy of the excitation energies derived from the LR-TDDFT methods in common use nowadays deteriorates with the size of the investigated system.[34−36] The established wave-function-based methods of quantum chemistry have the potential to reach the desired accuracy level for each of the two components of the spectral shift, that is, the excitation energy for the isolated chromophore and that of the chromophore in the complex. They can be used, in principle, without assuming that the errors are correlated. Using such methods is, however, not practical due to the computational effort needed to obtain the total energies (ground and excited state) at the equilibrium

TABLE 1: Contributions to the Spectral Shift Effect of Inserting the Linker Molecule (B) into the H-Bonded Chain Consisting of *cis*-7-Hydroxyquinoline and the Ligand Molecules (A and C), From the Linker in the Absence of Other Chain Members ($\delta\nu_{B(ABC)}$), Structural Changes Accompanying Inserting the Linker ($\delta\delta\nu_{geom}$), and Electronic Cooperativity of the Chain ($\delta\delta\nu_{el\text{-}coop}$)

ligands			$\delta\delta\nu_B$ and its components[a]				
A	C	B	$\delta\delta\nu_B^{exp}$ [b]	$\delta\delta\nu_B^{theor}$	$\delta\nu_{B(ABC)}$	$\delta\delta\nu_{geom}$	$\delta\delta\nu_{el\text{-}coop}$
NH_3	NH_3	NH_3	−315	−248	−336	348	−260
H_2O	H_2O	H_2O	−423	−298	−369	450	−379
CH_3OH	CH_3OH	CH_3OH	−461	−335	−384	391	−342
NH_3	NH_3	H_2O	−421	−417	−358	313	−372

[a] The shifts of the $\pi \rightarrow \pi^*$ excitations are given in [cm^{-1}]. [b] Reference 16.

geometries of the benchmark quality. It is worthwhile to point out that we consider this in our planned research studies of electronic excitations in clusters, which are larger in size than the ones considered in the present work.

For these reasons, we turned to the embedding strategy and especially to the nonempirical embedding formalism by Wesolowski and Warshel,[17,18] in which the embedding potential is expressed by means of a universal bifunctional depending on the two electron densities, that of the environment and that of the embedded subsystem (eq 3 in ref 23). For systems where the dynamic response of the environment can be neglected (neglect of dynamic response of the environment, NDRE approximation),[20] the quality of the excitation energies derived from embedding calculations does not deteriorate as is the case for supermolecular strategy.[36] Therefore, the differences between the excitation energy for the isolated chromophore and that for the chromophore in the complex can be expected to be of higher accuracy than the accuracy of the excitation energy of each of these two systems. The physical reason for this is due to the fact that the spectral shifts calculated in this way arise from the embedding potential perturbing the isolated chromophore. The applied orbital-free embedding potential possesses several exact features; (i) it obeys the correct dissociation limit, (ii) it reaches the dissociation limit in the exact way because it comprises the Coulombic component which dominates at long-range, and (iii) it includes the Pauli repulsion component, which, although not exact, was shown to be sufficiently accurate in cases where the electron densities of the chromophore and those of the environment do not overlap significantly, as is the case for hydrogen-bonded systems.[20] Indeed, practical examples show that these features of the embedding potential applied to calculate spectral shifts result in desired improvement compared to the supermolecular strategy to obtain the shifts.[36] For clusters comprising acetone and several water molecules, the lowest excitation energy derived from suopermolecular LR-TDDFT calculations changes in an erratic way if the number of water molecules in the cluster increases from 2 to 20. The "jumps" in this energy exceed the accuracy needed in our studies. Applying the embedding strategy to the same clusters leads to very stable results (see Figures 2−4 in ref 36). Focusing on spectral shifts of the 600−2000 cm^{-1} magnitude, the embedding strategy can be expected to be more adequate for studies of spectral shifts and their differences for systems comprising the same chromophore in different environments. It is worthwhile to note that the accuracy of the excitation energies derived from embedding and supermolecular calculations is essentially the same for small intermolecular clusters.[20] Turning back to the assumed NDRE approximation,[20] the adequacy of this assumption is strongly system-dependent. For complexes formed by similar molecules, the excitations are coupled, and the complete formalism combining orbital-free embedding and LR-TDDFT introduced in ref 19 should be applied. Indeed, Neugebauer[27] introduced a computational method in which selected coupled excitations are taken into account and demonstrated cases where NDRE is not adequate. (The NDRE calculations are refereed to as FDEu, that is, frozen density embedding uncoupled, in ref 27). For the systems considered in this work, we do not consider coupling between excitations in 7HQ and in the hydrogen-bonded chains because they absorb in different spectral regions.

Below, we outline only the key elements of the applied computational protocol. The relaxed two ground-state densities, that is, that of the chromophore (7HQ) and that of its environment (ligands), are obtained from a coupled set of one-electron equations (eqs 20 and 21 of ref 17). The freeze-and-thaw procedure[23] is used for this purpose. The orbitals in each set (occupied and nonoccupied) are localized in the respective subsystems (monomer expansion of electron densities referred to as KSCED(m) in ref 28), which is the default option in ADF2008 and which is described in detail in ref 28. Such a restriction on variational calculations is adequate in the absence of covalent bonds between subsystems and/or charge-transfer between subsystems.[18] These sets of orbitals are used in subsequent LR-TDDFT calculations in a different way. Whereas the ones corresponding to the chromophore are used in the general framework of LR-TDDFT calculations[21] with the response kernel modified to reflect the kinetic energy component of the effective potential,[20] the relaxed orbitals (occupied) corresponding to the environment are used only to derive the electron density of the environment and not contribute to the dynamic response of the system (NDRE approximation).

The applied monomer expansion of electron densities localizes the dynamic response of the chromophore which lies at the origin of the desired elimination of spurious electronic excitations involving the environment (see the relevant discussion in ref 36). The excitation energies were calculated using the ADF2008 code[30] with the following control parameters: Slater-type atomic orbitals (TZ2P), integration parameter 6.0, the GGA97[29] approximant for the nonadditive kinetic-energy-dependent part of the embedding potential, the PW91[31] approximant for the exchange-correlation-dependent part of the total orbital-free embedding potential, and the SAOP potential[32] for the part of the total potential representing the exchange-correlation potential of the embedded subsystem. The eigenvectors of the response matrix in LR-TDDFT calculations were obtained using a tough convergence criteria (TOLERANCE 1e-10).

The ground-state equilibrium geometry for the investigated complexes is obtained following the computational protocol described in detail in ref 26, in which local density approximation as applied for all needed functionals and potentials and the ground-state energy and density of the system is obtained from fully variational freeze-and-thaw calculations. A representative sample of benchmark results is provided in ref 26 and

TABLE 2: Contributions to the Spectral Shift Effect of Inserting the Linker Molecule (B in Figure 1) into the H-Bonded Chain Consisting of *cis*-7-Hydroxyquinoline and the Ligand Molecules (A and C), From the Linker in the Absence of Other Chain Members ($\delta\nu_{B(ABC)}$), Structural Changes Accompanying Inserting the Linker ($\delta\delta\nu_{geom}$), and Electronic Cooperativity of the Chain ($\delta\delta\nu_{el\text{-}coop}$)[a]

ligands			$\delta\delta\nu_B$ and its components[b]				
A	C	B	$\delta\delta\nu_B^{exp}$ [c]	$\delta\delta\nu_B^{theor}$	$\delta\nu_{B(ABC)}$	$\delta\delta\nu_{geom}$	$\delta\delta\nu_{el\text{-}coop}$
NH_3	NH_3	NH_3	−315	−191	−285	298	−204
H_2O	H_2O	H_2O	−423	−281	−314	358	−325
CH_3OH	CH_3OH	CH_3OH	−461	−384	−360	285	−309
NH_3	NH_3	H_2O	−421	−303	−320	276	−259

[a] Geometries from ref 16. [b] The shifts of the $\pi \rightarrow \pi^*$ excitations are given in [cm^{-1}]. [c] Reference 16.

compared to benchmark ab initio results collected in the database by Zhao and Truhlar.[33] In a set of hydrogen-bonded dimers of relevance for this work, the average deviations between the intermolecular distances obtained using such a protocol applied in the present work and the reference benchmark data are in the 0.1 Å range. The largest ones occur for the NH_3-NH_3 (−0.13 Å) and HCOOH−HCOOH dimers (0.11 Å). For the water−water and ammonia−water dimers, the deviations amount to only 0.02 Å. Such a precision in the identification of the equilibrium structure is sufficient for determination of environment-induced spectral shifts considered in the present work.

Results and Discussion

Table 1 collects the numerical values of $\delta\delta\nu_B$. The overall accuracy of the calculated shifts is rather good (see columns 4 and 5 in Table 1).The maximum difference between $\delta\delta\nu_B$ derived from the spectroscopic measurements and that from the applied computational protocol is 125 cm^{-1}. Such a discrepancy is rather small in view of the following factors: the vertical excitations picture in interpretation of experimental data; the chosen approximations for the density functional for the exchange-correlation and nonadditive kinetic energy contribution to the energy and to the effective potential needed in the determination of the equilibrium geometry; the chosen approximations for the density functional for the exchange-correlation and nonadditive kinetic energy contribution to the energy, to the effective potential, and to the response kernel and neglect of dynamic response of the environment in the determination of the vertical excitation energies; and other technical details such of the basis sets, grids, solver of the Kohn−Sham and Casida equations, and so forth.

The overall good accuracy of the calculated values of $\delta\delta\nu_B$ justifies a more detailed analysis of contributions to this quantity defined in the Introduction. The electronic cooperativity and the direct effect of the linker contribute to $\delta\delta\nu_B$ and both contributions always have a negative sign. Despite the fact that the linker does not interact directly with the chromophore in any of the complexes considered, its contribution ($\delta\nu_{B(ABC)}$ in Table 1) is not negligible. The contribution arising from the geometry relaxation always has a sign that is opposite to that of the spectral shift. All three contributions are considerable, and none appears to be dominant. It is interesting to note that the spectral shift contributions due to the inserted linker ($\delta\nu_{B(ABC)}$) and that due to the geometrical relaxation following introduction of the linker ($\delta\delta\nu_{geom}$) are opposite in sign. The relative importance of various contributions to $\delta\delta\nu_B$ is similar in all four considered hydrogen-bonded chains. Obviously, the numerical values reported in Table 1 depend on the geometry of the two- or three-member chains, which are taken from computations and not from experiment. It is interesting, therefore, to verify whether the obtained picture concerning the relative importance of various contributions to $\delta\delta\nu_B$ is general, that is, not specific for the considered geometries. To this end, $\delta\delta\nu_B$ as well as its components were recalculated using other methods to derive equilibrium geometries. For instance, for geometries optimized using the DFT-based method reported in ref 16, the corresponding spectral shifts are collected in Table 2 and show essentially the same trends. It is worthwhile to note that the overall agreement between $\delta\delta\nu_B$ derived from experiment and that from calculations is slightly worse for this set of geometries.

TABLE 3: Nonadditivity of the Dipole Moments (In Debye) of the Hydrogen-Bonded Chain[a]

ligands			dipole moment		
A	C	B	$\lvert\vec{\mu}_{ABC}\rvert$	$\lvert\vec{\mu}_{AC}+\vec{\mu}_B\rvert$	$\lvert\vec{\mu}_{ABC}-\vec{\mu}_{AC}-\vec{\mu}_B\rvert$
NH_3	NH_3	NH_3	4.71	2.89	1.97
H_2O	H_2O	H_2O	5.13	2.81	2.35
CH_3OH	CH_3OH	CH_3OH	5.81	3.11	2.73
NH_3	NH_3	H_2O	5.66	3.46	2.56

[a] The $\vec{\mu}_{ABC}-\vec{\mu}_{AC}-\vec{\mu}_B$ is the dipole moment arising from the mutual polarization of the induced electric dipole of the linker molecule (B) and the molecules at the end of the chain (A and C). Geometries of each considered system, full chain (ABC), chain without the linker (AC), and the linker (B), are as the equilibrium geometry of the 7HQ+ABC cluster.

The significant role of the electronic coupling between the two ends of the chain reflected in the magnitude of $\delta\delta\nu_{el\text{-}coop}$ defined in eq 2 calls for further analysis of its origin. In the language of commonly used decomposition schemes for the intermolecular interaction energy, $\delta\delta\nu_{el\text{-}coop}$ can be expected to originate from the nonadditivity of the induction and dispersion contributions. The analysis of the dipole moment of the chain indicates that the effect of induced dipoles on $\delta\delta\nu_{el\text{-}coop}$ is significant. For instance, the total dipole moment of the $3(NH_3)$ chain is 4.7 D, whereas the sum of the dipole moment of the $2(NH_3)$ chain (AC) and that of the linker NH_3 (B) is 2.9 D. The induced dipole moment arising from interactions between AC and B components of the chain is thus 2.0 D (i.e., about 38% of the total dipole moment of the three-membered chain). The induced dipole moments of the other three systems are collected in Table 3 showing similar trends.

It is well-known that the cooperativity of hydrogen-bonded chains affects the ground-state properties and leads to strengthening of the hydrogen bond as the chain elongates.[8,12] It is worthwhile, therefore, to supplement the analysis of the cooperativity of hydrogen-bonded chains made for the excited state with a similar analysis for a ground-state property. The total energies at the considered geometries are also available and allow one to address the issue of cooperativity in interactions between *cis*-7HQ and the molecules hydrogen-bonded to it. The cooperative contributions to the interaction energy due to the insertion of the linker evaluated using our method are collected

TABLE 4: Cooperative Component of the Interaction Energy ($\delta\delta E_B^{theor}$) and Its Contributions Due to Direct Interactions between *cis*-7HQ and the Linker ($\delta E_{B(ABC)}$), Geometrical Relaxation Following the Insertion of the Linker ($\delta\delta E_{geom}$), and the Electronic Cooperativity ($\delta\delta E_{el\text{-}coop}$)

ligands			$\delta\delta E_B^{theor}$ and its components[a]			
A	C	B	$\delta\delta E_B^{theor}$	$\delta E_{B(ABC)}$	$\delta\delta E_{geom}$	$\delta\delta E_{el\text{-}coop}$
NH_3	NH_3	NH_3	−4.72	−2.48	2.91	−5.15
H_2O	H_2O	H_2O	−7.05	−2.61	3.38	−7.81
CH_3OH	CH_3OH	CH_3OH	−7.87	−2.76	2.91	−8.02
NH_3	NH_3	H_2O	−6.05	−2.58	2.79	−6.26

[a] The energies are given in [kcal/mol].

in Table 4. The same convention for the contributions to the interaction energy as the one used for spectral shifts is applied here; the symbol δE (interaction energy) replaces $\delta\nu$ in the definitions of the discussed quantities and in the table. The electronic cooperativity provides a significant contribution to the energy of the interaction between the chain and the *cis*-7HQ molecule. Although the linker does not interact directly with *cis*-7HQ via a hydrogen bond, the electronic cooperativity provides additional stabilization of the system by an energy amount exceeding that of one additional hydrogen bond of the N−H···N type (about 5 kcal/mol or more). The electronic cooperativity of the hydrogen-bonding chains appears, therefore, to be the major factor in both ground- and excited-state properties of such systems.

Turning back to the LR-TDDFT results, we note that this strategy provides as the direct result the vertical excitation energies and the oscillator strengths of corresponding electronic transitions without, however, constructing the excited-state wave function. Nevertheless, eigenvectors of the response matrix evaluated in LR-TDDFT originate frequently from a contribution of only one pair of orbitals (one occupied and one unoccupied). In such a case, it is worthwhile to use such a pair in labeling. Moreover, in such cases, the difference between eigenvalues of the corresponding orbitals provides a useful simple estimate of the excitation energy. In the considered case, one pair of orbitals (HOMO and LUMO) provides the dominant contribution to the eigenvector (as much as 90%). These orbitals have π character. Consequently, we focused the analysis on these two orbitals. The orbital energies for the considered systems are collected in Table 5. The HOMO−LUMO gap in all of the complexes and clusters always decreases relative to the HOMO−LUMO gap of the isolated *cis*-7HQ chromophore. The magnitude of the decrease is between −1.4 and −8.2% and increases with the number of solvent molecules. Interestingly, solvation always destabilizes the HOMO relative to that of the isolated *cis*-7HQ (typically by −0.7 to −4.7%). The effect of solvation on the LUMO is not systematic; both increases and decreases are found. The shifts of the LUMO are about half that of the HOMO. As far as the shapes of these orbitals are concerned, they are not noticeably affected by the interactions with the environment (data not shown).

TABLE 5: Environment-Induced Shifts of the Orbital Energies (in [eV])[a]

ligands			shifts in the orbital energies		
A	*C*	*B*	$\Delta\varepsilon_{HOMO}$	$\Delta\varepsilon_{LUMO}$	$\Delta\varepsilon_{LUMO} - \Delta\varepsilon_{HOMO}$
NH_3	NH_3	NH_3	0.435	0.216	−0.219
	NH_3[b]		0.133	0.087	−0.046
NH_3[b]		NH_3[b]	0.351	0.192	−0.159
NH_3[c]		NH_3[c]	0.405	0.212	−0.193
H_2O	H_2O	H_2O	0.116	−0.114	−0.230
	H_2O[d]		0.094	0.043	−0.051
H_2O[d]		H_2O[d]	0.076	−0.078	−0.154
H_2O[e]		H_2O[e]	0.113	−0.086	−0.199
CH_3OH	CH_3OH	CH_3OH	0.193	−0.056	−0.249
	CH_3OH[f]		0.068	0.014	−0.054
CH_3OH[f]		CH_3OH[f]	0.182	0.007	−0.175
CH_3OH[g]		CH_3OH[g]	0.186	−0.027	−0.213
NH_3	H_2O	NH_3	0.394	0.158	−0.236
	H_2O[h]		0.122	0.073	−0.049
NH_3[h]		NH_3[h]	0.350	0.187	−0.163

[a] For the isolated *cis*-7HQ molecule, the orbital energies are ε_{HOMO} (*cis*-7HQ) = −9.737 eV, ε_{LUMO} (*cis*-7HQ) = −6.435 eV, and ε_{LUMO} (*cis*-7HQ)−ε_{HOMO} (*cis*-7HQ) = 3.302 eV. [b] $3NH_3$ geometry. [c] $2NH_3$ geometry. [d] $3H_2O$ geometry. [e] $2H_2O$ geometry. [f] $3CH_3OH$ geometry. [g] $2CH_3OH$ geometry. [h] $NH_3-H_2O-NH_3$ geometry.

Conclusions

The recently reported laser resonant two-photon ionization UV spectra of small clusters comprising the *cis*-7-hydroxyquinoline molecule and other molecules capable of hydrogen bonding[16] provide a new manifestation of the hydrogen-bond cooperativity. The insertion of a linker molecule in the middle of the hydrogen-bonded chain affects significantly the optical excitation energies of *cis*-7-hydroxyquinoline. This effect, which can be measured experimentally and which is denoted by $\delta\delta\nu_B^{exp}$, is not negligible. Its magnitude is on the order of 400 cm^{-1}, whereas the entire effect of the environment on these excitations is smaller than 2200 cm^{-1}. Such manifestation of hydrogen-bonding cooperativity could be expected in view of the known effects of the hydrogen-bonding cooperativity on ground-state properties, for example, the additional infrared band red shift of the donor asymmetric stretching vibration and the additional increase of the hydrogen-bond strength. Since the hydrogen-bond donor and acceptor properties of either end of the chain are strengthened, the effect of these groups on orbitals (occupied and unoccupied Kohn−Sham orbitals, and consequently the properties derived from them) of the chromophore can be expected also to be reinforced.

In the present work, we investigate the origin of $\delta\delta\nu_B^{exp}$ by evaluating the components of its computational counterpart $\delta\delta\nu_B^{theor}$. For the four investigated systems, $\delta\delta\nu_B^{theor}$ is close to the experimental value, and an important contribution to this quantity originates from the electronic coupling between the ends of the chain, which is enhanced by the presence of the linker. The importance of this electronic contribution seems to be a general feature of the considered chains. The changes of the geometry accompanying the insertion of the linker into the chain decrease the magnitude of the spectral shift, whereas the electronic cooperativity increases it. The fact that the observed cooperative effect correlates well with its electronic component in all considered systems and for two sets of similar but not identical geometries indicates that the electronic coupling reflected in the magnitude of the $\delta\delta\nu_{el\text{-}coop}$ defined in eq 2 should be considered an important factor also in cases where the geometry of the chain can be subject to some steric constraints, as is the case in biomolecules.

Acknowledgment. T.W. and S.L. acknowledge the support of Swiss National Science Foundation (Projects 200020-116760, 200020-124817/1, and 200020-113798).

Supporting Information Available: Cartesian coordinates of the considered complexes, equilibrium geometries from

subsystem DFT calculations (freeze-and-thaw), and the equilibrium DFT(B3LYP) geometries used in ref 16 and in this work for reference purposes. This material is available free of charge via the Internet at http://pubs.acs.org.

References and Notes

(1) Liu, K.; Cruzan, J. D.; Saykally, R. J. *Science* **1996**, *271*, 929.

(2) Anex, D. S.; Davidson, E. R.; Douketis, C.; Ewing, G. E. *J. Phys. Chem.* **1988**, *92*, 2913.

(3) Jucks, K. W.; Miller, R. E. *J. Phys. Chem.* **1988**, *88*, 2196.

(4) Yang, X.; Kerstel, E. R. T.; Scoles, G.; Bemish, R. J.; Miller, R. E. *J. Chem. Phys.* **1995**, *103*, 8828.

(5) Nauta, K.; Miller, R. E. *Science* **1999**, *283*, 1895.

(6) Ohno, K.; Okimura, M.; Akai, N.; Katsumoto, Y. *Phys. Chem. Chem. Phys.* **2005**, *7*, 3005.

(7) Sakota, K.; Kageura, Y.; Sekiya, H. *J. Chem. Phys.* **2008**, *129*, 054303.

(8) Ojamae, L.; Hermansson, K. *J. Phys. Chem.* **1994**, *98*, 4271.

(9) Karpfen, A. *J. Phys. Chem.* **1996**, *100*, 13474.

(10) Karpfen, A. *J. Phys. Chem. A* **1998**, *102*, 9286.

(11) Buckingham, A. D.; Del Bene, J. E.; McDowell, S. A. C. *Chem. Phys. Lett.* **2008**, *463*, 1.

(12) Karpfen, A. *Adv. Chem. Phys.* **2002**, *123*, 469.

(13) Guo, H.; Gresh, N.; Roques, B. P.; Salahub, D. R. *J. Phys. Chem. A* **2000**, *104*, 9746.

(14) Domcke, W.; Sobolewski, A. L. *Science* **2003**, *302*, 1693.

(15) Tanner, C.; Manca, C.; Leutwyler, S. *Science* **2003**, *302*, 1736.

(16) Thut, M.; Tanner, C.; Steinlin, A.; Leutwyler, S. *J. Phys. Chem. A* **2008**, *112*, 5566.

(17) Wesołowski, T. A.; Warshel, A. *J. Phys. Chem.* **1993**, *97*, 8050.

(18) Wesolowski, T. A. One-electron equations for embedded electron density: challenge for theory and practical payoffs in multi-level modelling of soft condensed matter. In *Computational Chemistry: Reviews of Current Trends*; Leszczynski, J., Ed.; World Scientific: River Edge, NJ, 2006; Vol. X, pp 1−82.

(19) Casida, M. E.; Wesolowski, T. A. *Int. J. Quantum Chem.* **2004**, *96*, 577.

(20) Wesolowski, T. A. *J. Am. Chem. Soc.* **2004**, *126*, 11444.

(21) Casida M. E. Time-Dependent Density Functional Response Theory of Molecular Systems: Theory, Computational Methods, and Functionals. In *Recent Developments and Applications of Modern Density Functional Theory*; Seminario, J. M., Ed.; Elsevier Science B.V.: New York, 1996, Vol. 4, pp 391−439.

(22) Dreuw, A.; Head-Gordon, M. *Chem. Rev.* **2005**, *105*, 4009.

(23) Wesolowski, T. A.; Weber, J. *Chem. Phys. Lett.* **1996**, *248*, 71.

(24) Hohenberg, P.; Kohn, W. *Phys. Rev. B* **1964**, *136*, 864.

(25) Kohn, W.; Sham, L. J. *Phys. Rev.* **1965**, *140*, A1133.

(26) Dulak, M.; Kaminski, J.; Wesolowski, T. A. *J. Chem. Theory Comput.* **2007**, *3*, 735.

(27) Neugebauer, J. *J. Chem. Phys.* **2007**, *126*, 134116.

(28) Wesolowski, T. A.; Chermette, H.; Weber, J. *J. Chem. Phys.* **1996**, *105*, 9182.

(29) Wesolowski, T. A.; Chermette, H.; Weber, J. *J. Chem. Phys.* **1996**, *105*, 9182.

(30) *ADF2008 suite of programs*; Theoretical Chemistry Department, Vrije Universiteit: Amsterdam, The Netherlands; http://www.scm.com (2008).

(31) Perdew J. P., Wang Y. In *Electronic Structure of Solids*; Ziesche, P. E., Eschrig, H., Eds.; Academie Verlag: Berlin, Germany, 1991; p 11.

(32) Gritsenko, O. V.; Schipper, P. R. T.; Baerends, E. J. *Chem. Phys. Lett.* **1999**, *302*, 199.

(33) Zhao, Y.; Truhlar, D. G. *J. Chem. Theory Comput.* **2005**, *1*, 415.

(34) Dreuw, A.; Head-Gordon, M. *J. Am. Chem. Soc.* **2004**, *126*, 4007.

(35) van Gisbergen, S. J. A.; Schipper, P. R. T.; Gritsenko, O. V.; Baerends, E. J.; Snijders, J. G.; Champagne, B.; Kirtman, B. *Phys. Rev. Lett.* **1999**, *83*, 694.

(36) Neugebauer, J.; Louwerse, M. J.; Baerends, E. J.; Wesolowski, T. A. *J. Chem. Phys.* **2005**, *122*, 094115.

JP906483Z